



UNIVERSITEIT•STELLENBOSCH•UNIVERSITY
jou kennisvenoot • your knowledge partner

*A high performance concentric magnetic gear
(repository copy)*

Article:

Mathee, A., Gerber, S., Wang, R-J., (2015) A high performance concentric magnetic gear", *Proc. of the Southern African Universities Power Engineering Conference*, (SAUPEC), Johannesburg, South Africa, pp. 203--207, 28-29 January 2015

Reuse

Unless indicated otherwise, full text items are protected by copyright with all rights reserved. Archived content may only be used for academic research.

A HIGH PERFORMANCE CONCENTRIC MAGNETIC GEAR

A. Matthee*, S. Gerber* and R-J Wang*

* Dept. of Electrical and Electronic Engineering, Stellenbosch University, Stellenbosch 7600
E-mail: alexandermatthee@gmail.com; sgerber@sun.ac.za; rwang@sun.ac.za

Abstract: This paper is concerned with the design improvement of a previously designed magnetic gear with emphasis on performance optimization and the mitigation of end-effects. The performance analysis results show approximately 70% reduction in losses at full load and a 40% increase in maximum torque capability. New flux modulator manufacturing techniques, which yielded great results, are discussed.

Key words: Magnetic gears, end-effects, permanent magnet, design optimization

1. INTRODUCTION

Magnetic gears are receiving more attention in recent years. Among different types of magnetic gears, the concentric magnetic gear (MG) has been the focus of research and development. With a torque density comparable to mechanical gears, concentric MGs also demonstrate other distinct benefits such as high efficiency, low noise, low maintenance and overload protection. The potential applications for this novel gear technology include industrial drives, material handling, electric vehicles and wind turbine applications [1, 2]. This paper reports the design improvements of a previously designed concentric MG [3], which shows inferior torque and efficiency performance when compared with the design values. Design recommendations mentioned in [4] as well as other possible solutions will be investigated.

2. PRINCIPLE OF OPERATION

High-order magnetic flux harmonics are usually undesirable as they are the sources of torque ripple or loss, heating and decreased efficiency in electrical machines. In the case of the magnetic gear, harmonics are used to an advantage by making use of specific characteristics of these harmonics to realize a gear action between input and output rotors. Fig. 1 displays a cross-sectional view of a concentric-type magnetic gear, which consists of three concentric elements, namely, outer low-speed (LS) rotor, inner high-speed (HS) rotor and a flux modulator between them. If the flux modulator is kept stationary, the gear ratio G_r is governed by the following equation [5]:

$$G_r = \frac{q - p_h}{p_h} = \frac{p_l}{p_h} \quad (1)$$

where q is the number of modulator segments, p_l and p_h are the pole-pairs of the LS and HS rotors respectively. The fundamental operation principle of a magnetic gear is the modulation of fluxes from both high and low speed rotors. Fig. 2 shows the flux density waveform generated only by the magnets of the LS rotor in the HS side air-gap and its harmonic composition. It can be clearly seen that due to flux modulation there exists a prominent 2nd order space harmonic in the HS air-gap, which matches the HS

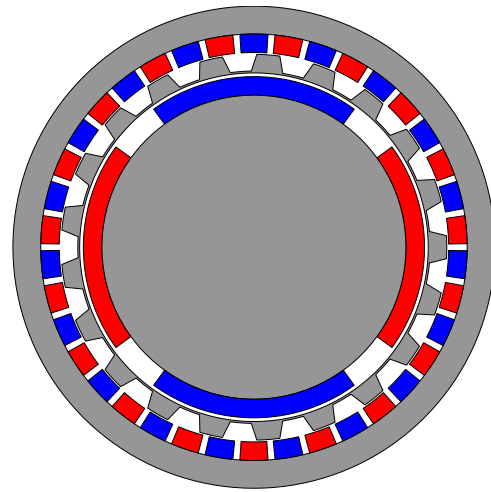


Figure 1: The layout of a concentric magnetic gear

pole pairs. Similarly the air-gap flux density waveform generated by only HS magnets in the LS air-gap and its harmonic composition is shown in Fig. 3. It can be observed that a large 21st order space harmonic, which corresponds to the LS pole-pairs, is present in the LS side air-gap as a result of flux modulation.

3. DESIGN IMPROVEMENTS

3.1 Problems with the Previous Design

The previously developed magnetic gear demonstrates relatively poor performance when compared with the calculated results. A recent study [4] shows that the performance reduction of the MG is mainly caused by the following design issues:

- the severe end leakage flux in the supporting structure not only reduces the magnitude of the torque producing harmonics, but also causes excessive eddy current loss in the end plates, which reduces the gear efficiency
- the stack length of the flux modulator is longer than the active PM length, which increases the flux leakage in the end region and reduces the peak torque capacity

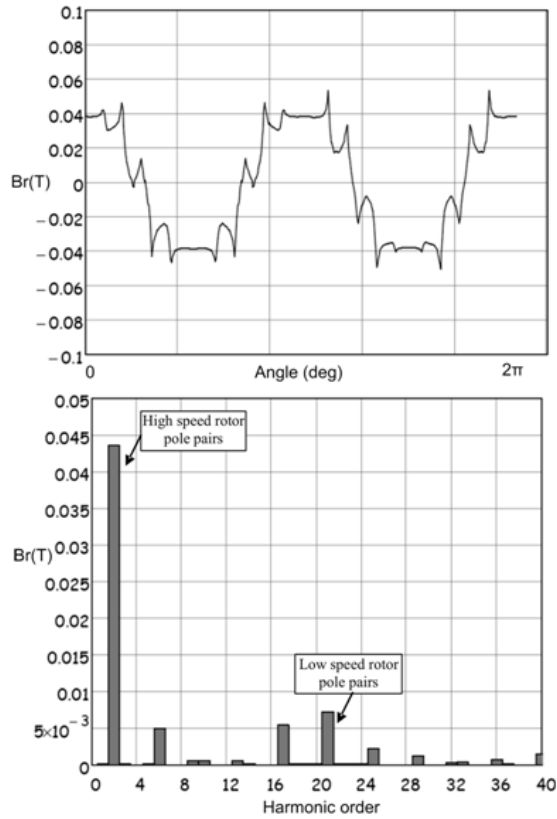


Figure 2: Flux density in HS Air-gap due to LS magnets [1]

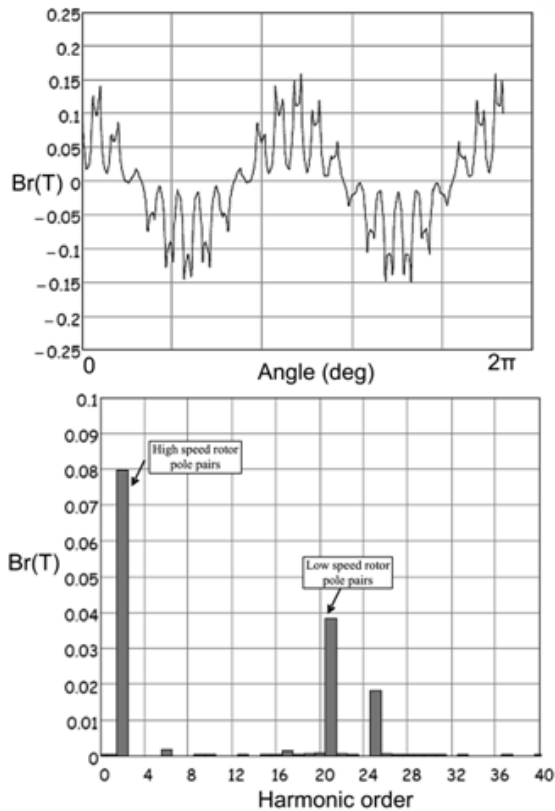


Figure 3: Flux density in LS Air-gap due to HS magnets [1]

Table 1 gives the key design specifications of the previously developed magnetic gear [3].

Table 1: Design specs of the magnetic gear prototype

Parameter	Value
Pole pairs on high speed rotor	2
Pole pairs on low speed rotor	21
Number of stator segments or pole-pieces	23
Outer radius of low speed yoke, mm	57.5
Inner radius of low speed yoke, mm	52.5
Outer radius of stator segments, mm	52
Inner radius of stator segments, mm	45
Outer radius of the high speed rotor, mm	44.3
Stack length, mm	40
Permanent magnet thickness, mm	5
Permanent magnet grade	N35

3.2 Objectives and Design Approach

The objective of the design improvements is to optimize the output torque capability of the previously developed magnetic gear. 2D FEM simulations have been applied to calculate the peak torque of the MG and analyze the flux distribution associated with different flux modulator designs. Several flux modulator topologies are evaluated and the most promising one is then selected for further design optimization. The optimum design obtained from 2D FEM optimization is modeled using 3D FEM for more accurate performance computation.

A commercial optimization software VisualDoc has been used together with SEMFEM, an in-house developed FEM package, for the optimization of the magnetic gear. A Python script is used to read the design variables and update the FE model. Fig. 4 shows the flowchart of the design optimization process. The optimized modulator design illustrated in Fig. 5 achieves a peak torque of 54.6 Nm (based on 2D FE calculation), which is about 2% improvement when compared with the previous design.

3.3 3D FEM Analysis

Since a typical magnetic gear exhibits no magnetic periodicity, a full FE model is required, which implies that FE modeling of an MG in 2D is already computationally expensive, not even to mention 3D FE analysis. 3D FEM simulation is used only to verify 2D FEM design as these can be very computationally expensive. Since 2D FEM simulations neglects end-effects of a magnetic gear, 3D FE simulations always result in a lower but more accurate torque output value. The 3D FEM model of the final design can be seen in Fig. 6. The previously constructed prototype has an extended stack length of 45 mm, which intensifies the flux leakage in the end regions, causing a reduction in the peak torque. The improved design, with an optimal stack length of 40 mm, increases the peak torque to 48.6 Nm (3D FE results), a 9.95% increase over the previous prototype.

4. CONSTRUCTION OF THE PROTOTYPE

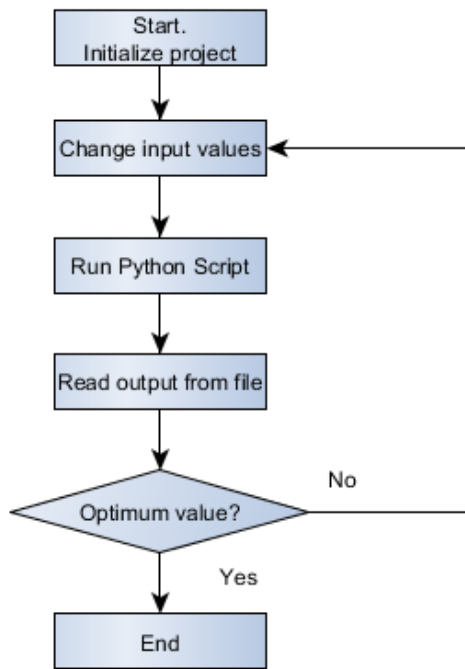


Figure 4: Flowchart of the optimization process

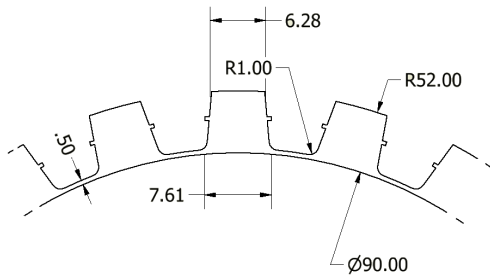


Figure 5: Section of the final modulator design

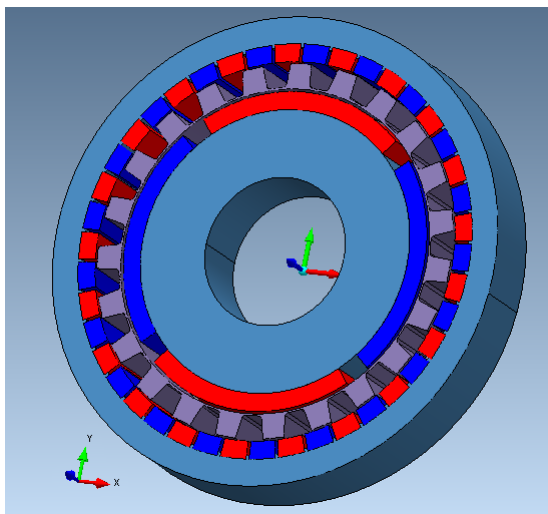


Figure 6: Auxiliary view of 3D FE model

The mechanical design changes have been effected with an aim to mitigate losses incurred in the gear due to end-effects. In the previous design the modulator was mounted directly on the mild steel high-speed cover plate as shown in Fig. 7, which has been identified as one of the major causes for excessive loss during high speed operation [4]. The new modulator design is constrained by the previous design's magnet layout. The magnets and shafts are re-used due to the limited time available to complete this project. The outer and inner radii of the modulator are therefore fixed but all other dimensions are free to be optimized. It has been shown in [4] that the thin bridges connecting the segments of the flux modulator increase the output torque and reduce unwanted harmonics. The final modulator retains this design feature.

In addition, a new casing is made from aluminum which has a much lower relative permeability. The cover plates of both high-speed and low-speed sides are remade using aluminum. The low speed side cover plate is slightly lengthened to better align the modulator to the magnets. This is necessary due to the newly added support ring. The low-speed yoke, which supports the low speed magnets, effectively shields the low speed cover plate from the majority of magnetic fields. The high speed cover plate and surrounding structure are the focus of the mechanical design improvement. As the casing has to support the modulator, which is a high flux density region, the casing is moved further away from the modulator segments by 15.5 mm. This increase in distance decreases the strength of magnetic fields that penetrate the casing (See sectional view of gear in Fig. 7).

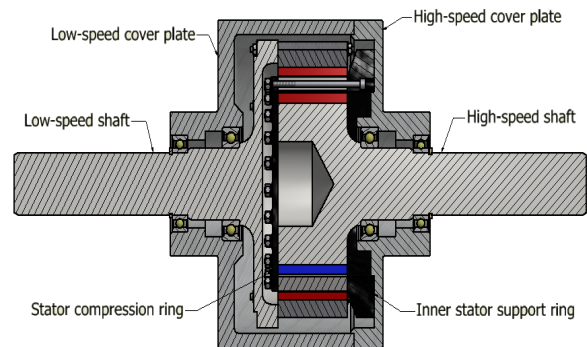


Figure 7: Sectional view of the final magnetic gear

The modulator, consisting of laminations, requires a mould to be positioned accurately. Previously the laminations were laser cut to specification and assembled on the mould before the epoxy bonding for added structural strength. A new process is followed whereby the lamination are cut larger than designed which allows a key groove to be added as shown in Fig. 8. This greatly simplifies the assembling process and allows the correction for possible dimensional imperfections. Once epoxy is applied and cured the entire modulator is machined to specification.

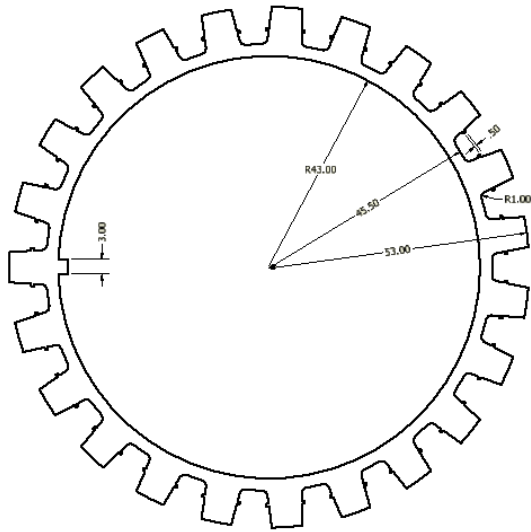


Figure 8: Cross-section of the final modulator design

The stainless steel rings previously used to compress and mount the modulator are replaced by Vesconite plastic supporting structures. Vesconite is a high load bearing plastic with dimensional stability but is also easy to machine. It is therefore chosen as the ideal non-magnetic material to use for supporting the modulator. The modulator inner support ring is mounted securely to the high-speed cover plate with 10 stainless steel bolts.

5. PERFORMANCE EVALUATION

In this section the experimental tests of the new magnetic gear prototype is described. Results obtained in these tests will be compared to those of the previously designed magnetic gear. Fig. 9 is a photo of the test setup.

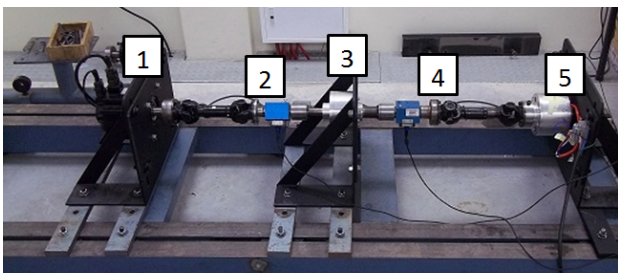


Figure 9: The test setup, where 1 - brushless DC motor drive, 2 - torque sensor, 3 - magnetic gear, 4 - torque sensor, 5 - pseudo direct drive generator as load machine.

5.1 No-Load Test

This test determines the no-load loss (including wind friction and core losses) in the magnetic gear. As shown in Fig. 10, the no-load loss of the previous magnetic gear is 157 W at 1700 rpm while this loss reduces to only 49 W at the same speed for the new gear design. This works out to be 68.7% reduction in losses at the mentioned speed. It is evident that the new magnetic gear prototype has much

reduced no-load loss when compared with the previously designed one.

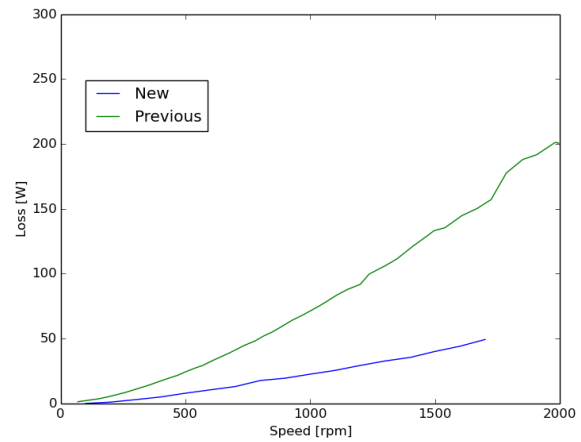


Figure 10: Comparison of no-load loss between the previous and the improved magnetic gears

5.2 Load Tests

The loss in a magnetic gear is mainly affected by its operation frequency and thus its rotational speed. The load placed on the gear has little effect on the losses of the gear. The load tests are performed at different speeds ranging from 100 rpm to 1700 rpm (on high speed side). At every speed interval the load is adjusted to vary the torque on the low speed shaft at intervals of 10 Nm starting at 10 Nm to a maximum value of 40 Nm. Fig. 11 shows the output power as a function of speed for different levels of output torque. The magnetic gear achieves a power output of 680 W at 160 rpm and 40 Nm torque.

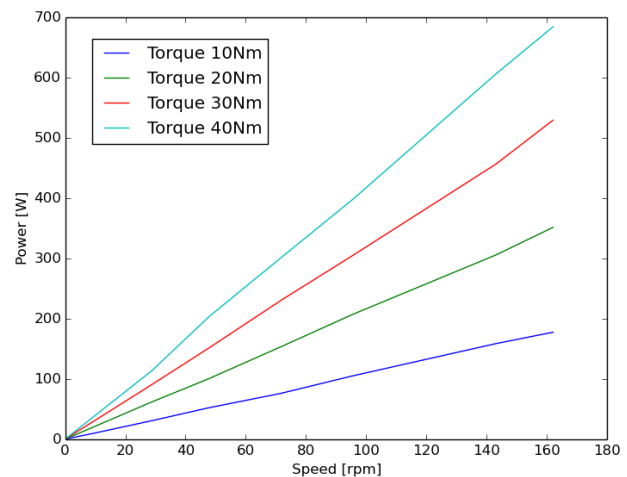


Figure 11: The output power of the magnetic gear as a function of speeds for different loads (on low speed side)

The efficiency map of the magnetic gear at different operation conditions is given in Fig. 12. It can be observed that the efficiency of the magnetic gear at 4 Nm and 1500 rpm (high speed side) is about 95%. Comparing with

the previous magnetic gear, the efficiency of the improved magnetic gear shows a marked improvement.

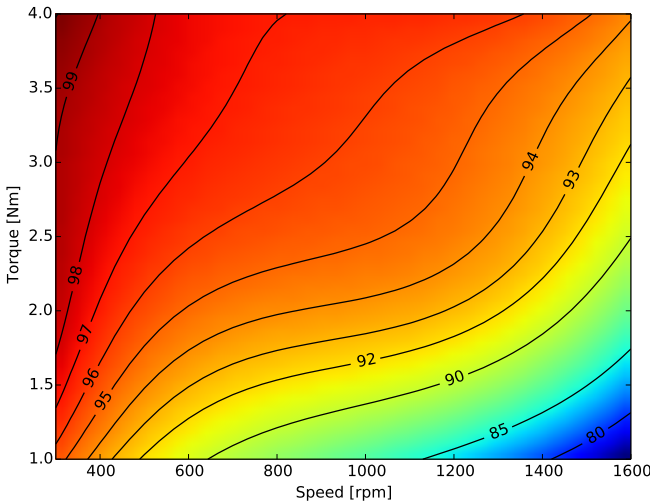


Figure 12: The efficiency map of the magnetic gear at different operation conditions (on high speed side)

5.3 Stall Torque

For the stall torque test the high-speed shaft of the magnetic gear is clamped and forced to a stationary position. A metal bar is attached to the low-speed side of the magnetic gear via a torque sensor to manually apply the torque. The stall torque is the maximum torque that can be transferred before the magnetic poles slip. This kind of pole-slipping under overload conditions offers inherent protection to a magnetic gear. The measured stall torque value of the new magnetic gear prototype is 46.2 Nm, which is about 13.2 Nm (or 40%) more than that of the previously designed magnetic gear [4]. Table 2 compares the measured and predicted stall torque values of the magnetic gear. It is clear that 3D FEM gives more accurate prediction than 2D FEM.

Table 2: Measured and predicted stall torque values

Method	Value	Diff%
Measured	46.2 Nm	-
3D FEM	48.6 Nm	5.2%
2D FEM	54.6 Nm	18.2%

6. CONCLUSION AND RECOMMENDATION

This paper describes the design improvements on a previously designed concentric magnetic gear. By optimizing the flux modulator and carefully considering the design aspects affecting 3D end-effects, the overall performance (efficiency and torque capability) of the magnetic gear has been significantly improved. The improved prototype has been constructed and experimentally evaluated. The measured results compare favorably with the predicted ones. The distinct features and high performance of magnetic gears make them an attractive alternative to conventional mechanical gears.

6.1 Recommendation for Future Work

Although the improved prototype shows a significant reduction in no-load loss, leakage magnetic fields are still present in the region of the high-speed casing that supports the modulator. Reducing this end leakage field will further improve the overall efficiency of the magnetic gear, especially at higher operation speeds. Possible solutions include increasing the distance between the modulator segments and the high-speed casing or constructing the entire high-speed casing from a non-magnetic material such as Vesconite.

Both 2D and 3D FEM simulations show that a slightly higher output torque can be achieved for the bridged modulator segments without the curved corners. These curved corners were added to the design to enhance the structural strength of the lamination, which in the end appears to be unnecessary.

For the previously constructed magnetic gear the N35H NdFeB magnets were used. Using stronger magnets in the design will easily improve the torque density of the magnetic gear by a significant margin.

ACKNOWLEDGMENT

This work was supported in part by Eskom Tertiary Education Support Program (TESP), Stellenbosch University and the National Research Foundation (NRF).

REFERENCES

- [1] R-J Wang, S. Gerber, "Magnetically geared wind generator technologies: Opportunities and challenges", *Applied Energy*, 136:817-826, Elsevier, 2014.
- [2] N. Niguchi, K. Hirata, M. Muramatsu, and Y. Hayakawa, "Transmission Torque Characteristics in a Magnetic Gear", *XIX International Conference on Electrical Machines (ICEM)*, 6p, Rome, Sept. 2010.
- [3] L. Brönn, R-J Wang, M.J. Kamper, "Development of a shutter type magnetic gear", *Proc. of the 19th Southern African Universities Power Engineering Conference*, pp.78-82, Wits University, Johannesburg, Jan. 2010.
- [4] S. Gerber and R-J. Wang, "Evaluation of a Prototype Magnetic Gear", *IEEE International Conference on Industrial Technology (ICIT)*, pp.319-324, Cape Town, Feb. 2013.
- [5] K. Atallah, S. Calverley, and D. Howe, "Design, analysis and realisation of a high-performance magnetic gear", *IEE Proc. Electric Power Applications*, 151(2):135-143, Mar. 2004.